Computer Assisted Methods in Engineering and Science, **22**: 99–114, 2015.

A 16-node locking-free Mindlin plate resting on two-parameter elastic foundation – static and eigenvalue analysis

Ryszard Buczkowski[1], Maciej Taczała[2], Michał Kleiber[3]

[1] *Maritime University of Szczecin*
Division of Computer Methods
Pobożnego 11, 70-507 Szczecin, Poland
e-mail: rbuczkowski@ps.pl

[2] *West Pomeranian University of Technology*
Piastów 41, 71-065 Szczecin, Poland
e-mail: maciej.taczala@zut.edu.pl

[3] *Institute of Fundamental Technological Research*
Polish Academy of Sciences
Pawińskiego 5B, 02-106 Warszawa, Poland
e-mail: mkleiber@ippt.pan.pl

The Pasternak elastic foundation model is employed to study the statics and natural frequencies of thick plates in the framework of the finite element method. A new 16-node Mindlin plate element of the Lagrange family and a 32-node zero-thickness interface element representing the response of the foundation are used in the analysis. The plate element avoids ill-conditioned behaviour due to its small thickness. In the case of the eigenvalue analysis, the equation of motion is derived by applying the Hamilton principle involving the variation of the kinetic and potential energy of the plate and foundation. Regarding the plate, the first-order shear deformation theory is used. By employing the Lobatto numerical integration in which the integration points coincide with the element nodes, we obtain the diagonal form of the mass matrix of the plate. In practice, diagonal mass matrices are often employed due to their very attractive time-integration schemes in explicit dynamic methods in which the inversion of the effective stiffness matrix as a linear combination of the damping and mass matrices is required. The numerical results of our analysis are verified using thin element based on the classical Kirchhoff theory and 16-node thick plate elements.

Keywords: Mindlin plate, two-parameter elastic foundation, Lobatto integration, bending and eigenvalue analysis.

1. Introduction

The analysis of thick or thin plates interacting with homogeneous or non-homogeneous foundation is a very important engineering problem. A large number of studies have been conducted on the bending and vibration of plates lying on an elastic foundation. In the paper by Omurtag et al. [1] the dynamic formulation of Kirchhoff plate resting on Pasternak foundation was analysed with mixed-type formulation using the Gâteaux derivative. The free vibration of rectangular clamped thick plates resting on the two-parameter elastic foundation was analysed in [2], where the Chebyschev polynomials multiplied by the boundary function were taken to satisfy the geometric boundary conditions of the plate and the Ritz method was used to derive the eigenvalue equations. Çelik and Saygun [3], Çelik and Omurtag [4], Ozgan and Omurtag [5], Ozgan and Daloglu [6] and Buczkowski and Torbacki [7, 8] presented the finite element technique where the material properties of soil are taken into account to incorporate the surrounding effect outside the plate. The rectangular elastic

plates resting on a tensionless Winkler foundation were analysed by Celep [9]. The static and dynamic analysis of a circular plate on a two-parameter tensionless foundation has been recently investigated using the Galerkin approximation technique by Celep and Güler [10]. The problem of tensionless elastic foundation under flexible rectangular Mindlin plates has been also studied by Mishra and Chakrabarti [11]. In the paper by Eratll and Aköz [12], a solution for Reissner plates on a Winkler foundation was formulated based on the Gâteaux derivative theory. Özçelikörs et al. [13] also used the Gâteaux differential method combined with the classical Hellinger-Reissner and Hu-Washizu variational formulations to obtain a solution for the interaction between orthotropic Kirchhoff plate and orthotropic Pasternak foundation. The mixed Galerkin-perturbation technique wa recently used by Shen [14] in an attempt to analyse the nonlinear bending of rectangular Reissner-Mindlin plates with free edges, resting on a Pasternak elastic foundation. In the paper by Feng and Owen [15], a coupled finite element and boundary element procedure for analysing a plate-foundation problem was described. In Sadecka [16] infinite elements were used to take into account the reaction of the ground outside the plate. The discrete singular convolution method was developed by Civalek and Acar [17] and Civalek and Ersoy [18] for the static analysis of the bending and free vibration of thick plates on a Pasternak foundation for different boundary conditions and arbitrary edges. In two papers by Akhavan et al. [19, 20] the authors, considering the first-order shear deformation theory, presented exact solutions for free vibrations and for the buckling analysis of rectangular Mindlin plates under in-plane loading while resting on a Pasternak foundation. The bending of plates resting on a Pasternak foundation was investigated by Zenkour et al. [21–23] and Vallabhan and Daloglu [24]. The authors in [21, 22] used the mixed first-order transverse (where both the displacements and stresses are considered arbitrary) or sinusoidal shear deformation [23] theories that do not require a shear correction factor.

Thick plate element performance depends on the ratio of thickness to length of the plate. When this ratio becomes extremely small, shear locking may occur. To avoid this shear locking in thick plates Özdemir [25] has recently developed a fourth- order 17-node Mindlin finite element that indicates excellent results for the static and dynamic analysis of thick plates resting on a Winkler foundation.

In the present paper, a Pasternak elastic foundation model is employed to study the bending and natural frequencies of a thick plate in the framework of the finite element method. A 16-node Mindlin plate element of the Lagrange family, which is free from shear locking, is used in the study. The effects of mid-plane stretching due to immovable ends on the deflection of the plate are neglected. The subspace iteration procedure is used in the paper to obtain eigenvalues and eigenvectors.

2. Formulation of the stiffness of the foundation and mass matrix of the plate

2.1. Mathematical relations

The equation of motion is derived by applying the Hamilton principle that requires the variation of the kinetic and potential energy of the plate and stiffeners considered during any time interval to equal zero:

$$\int_{t_1}^{t_2} (\delta U - \delta T)\, \mathrm{d}t = 0. \tag{1}$$

The potential energy in the case of eigenvibrations corresponds to the strain energy of the Reissner-Mindlin plate and the elastic foundation according to the formulation typical for the Pasternak model. Variation of the potential energy is given by [7]

$$\delta U = \int_{V_p} (\sigma_x \delta\varepsilon_x + \sigma_y \delta\varepsilon_y + \tau_{xy}\delta\gamma_{xy} + \tau_{xz}\delta\gamma_{xz}\tau_{yz}\delta\gamma_{yz})\,\mathrm{d}V + \int_{A_f} [k_0 w\delta w + k_1 (w_{,x}\delta w_{,x} + w_{,y}\delta w_{,y})]\,\mathrm{d}A, \tag{2}$$

where k_0 is the first, or Winkler foundation, parameter and k_1 is the second, or shear foundation parameter. The symbols $w_{,x}$ and $w_{,y}$ denote differentiation with respect to Cartesian coordinates x and y, respectively. For more details see [7].

Employing the Reissner-Mindlin formulation for the description of the plate deflection, three displacement functions are used: u_t and v_t for in-plane displacements and w_t for out-of-plane displacements.

Variation of the kinetic energy from t_1 to t_2

$$\int_{t_1}^{t_2} \delta T\,\mathrm{d}t = \int_{t_1}^{t_2}\int_{V_p} \rho (\dot{u}_t\delta\dot{u}_t + \dot{v}_t\delta\dot{v}_t + \dot{w}_t\delta\dot{w}_t)\,\mathrm{d}V\mathrm{d}t \tag{3}$$

can be integrated by parts as follows:

$$\int_{t_1}^{t_2}\int_{V_p} \rho (\dot{u}_t\delta\dot{u}_t + \dot{v}_t\delta\dot{v}_t + \dot{w}_t\delta\dot{w}_t)\,\mathrm{d}V\mathrm{d}t = \int_{V_p} \rho (\dot{u}_t\delta u_t + \dot{v}_t\delta v_t + \dot{w}_t\delta w_t)\,\mathrm{d}V\Big|_{t_1}^{t_2} - \int_{t_1}^{t_2}\int_{V_p} \rho (\ddot{u}_t\delta u_t + \ddot{v}_t\delta v_t + \ddot{w}_t\delta w_t)\,\mathrm{d}V\mathrm{d}t. \tag{4}$$

Variations of displacement functions must vanish at the limits of integration t_1 and t_2, hence

$$\int_{t_1}^{t_2} \delta T\,\mathrm{d}t = -\int_{t_1}^{t_2}\int_{V_p} \rho (\ddot{u}_t\delta u_t + \ddot{v}_t\delta v_t + \ddot{w}_t\delta w_t)\,\mathrm{d}V\mathrm{d}t. \tag{5}$$

Using the formulation of the displacement function for the first-order shear deformation theory (FSDT):

$$\begin{aligned} u_t &= u + z\theta_y, \\ v_t &= v - z\theta_x, \end{aligned} \tag{6}$$

where θ_x and θ_y are rotations of the normal to the undeformed midsurface around the x-axis and y-axis, respectively. For plates in bending, excluding in-plane effects ($u = 0$, $v = 0$):

$$\begin{aligned} u_t &= z\theta_y, \\ v_t &= -z\theta_x. \end{aligned} \tag{7}$$

So, from Eq. (5) using equations in (7), we arrive at

$$\int_{t_1}^{t_2} \delta T\,\mathrm{d}t = -\int_{t_1}^{t_2}\int_{V_p} \rho \left(z^2\ddot{\theta}_y\delta\theta_y + z^2\ddot{\theta}_x\delta\theta_x + \ddot{w}_t\delta w_t\right)\mathrm{d}V\mathrm{d}t, \tag{8}$$

where ρ is the material density.

Strains of the Mindlin-Reissner plate are given by

$$\varepsilon_x = z\theta_{y,x}, \qquad \varepsilon_y = -z\theta_{x,y},$$
$$\gamma_{xy} = z\left(\theta_{y,y} - \theta_{x,x}\right), \tag{9}$$
$$\gamma_{xz} = w_{,x} + \theta_y, \qquad \gamma_{yz} = w_{,y} - \theta_x.$$

Constitutive relationships are written in the following way:

$$\sigma_x = \frac{E}{1-\nu^2}\left(\varepsilon_x + \nu\varepsilon_y\right), \qquad \sigma_y = \frac{E}{1-\nu^2}\left(\varepsilon_y + \nu\varepsilon_x\right),$$
$$\tau_{xy} = G\gamma_{xy}, \qquad \tau_{xz} = \beta G\gamma_{xz}, \qquad \tau_{yz} = \beta G\gamma_{yz}, \tag{10}$$

where β is a shear correction factor which is equal to $\beta = 5/6$.

In the finite element approach, the same interpolation functions are used for displacements of the plate and the elastic foundation to maintain compatibility. Out-of-plane displacements, as well as rotations, are expressed in terms of the shape functions:

$$w = N_j w_j = N_{1j}^{(2)} d_j,$$
$$\theta_x = N_j \theta_{xj} = N_{2j}^{(2)} d_j, \tag{11}$$
$$\theta_y = N_j \theta_{yj} = N_{3j}^{(2)} d_j,$$

where $\mathbf{N}$ and $\mathbf{N}^{(2)}$ are the shape function matrices of the plate element (see Appendix A) and $\mathbf{d}$ is the nodal displacement vector

$$\mathbf{d} = \left[w_1 \;\; \theta_{x1} \;\; \theta_{y1} \;\; w_2 \;\; \theta_{x2} \;\; \theta_{y2} \;\; \ldots \;\; w_{16} \;\; \theta_{x16} \;\; \theta_{y16}\right]^{\mathrm{T}}. \tag{12}$$

The isoparametric approach is used in the present formulation. Therefore, the shape functions are given in natural coordinates, and their derivatives necessary for formulation of the stiffness matrix are evaluated by employing the chain rule and the determinant of the Jacobian matrix.

Employing equations in (11) to the original formulations of the Hamilton principle (Eqs. (2) and (8)) yields

$$\int_{t_1}^{t_2} \left[K_{jk} d_j + M_{jk} \ddot{d}_j\right] \delta d_k \mathrm{d}t = 0, \tag{13}$$

where K_{jk} is the stiffness matrix of the plate and elastic foundation while M_{jk} is the mass matrix of the plate.

Since Eq. (13) must be true for arbitrary variation of displacement and time interval $\mathrm{d}t$, it follows that

$$K_{jk} d_j + M_{jk} \ddot{d}_j = 0. \tag{14}$$

Assuming that the displacement is a harmonic function of time

$$d_j = d_j^{(0)} \sin \omega t, \tag{15}$$

Equation (14) becomes

$$\left(K_{jk} - \omega^2 M_{jk}\right) d_j^{(0)} = 0, \tag{16}$$

which is a standard eigenvalue problem.

The mathematical model for the static analysis can be formulated beginning with the principle of virtual work. In particular, the same stiffness matrix is then obtained and the term referring to the virtual work of external loading yields to the equivalent force vector (details can be found in [7 ,8]).

2.2. Stiffness matrix of the foundation

This part of the paper considers relationships used for deriving the stiffness matrix of the 32-node finite non zero-thickness foundation element, shown in Fig. 1.

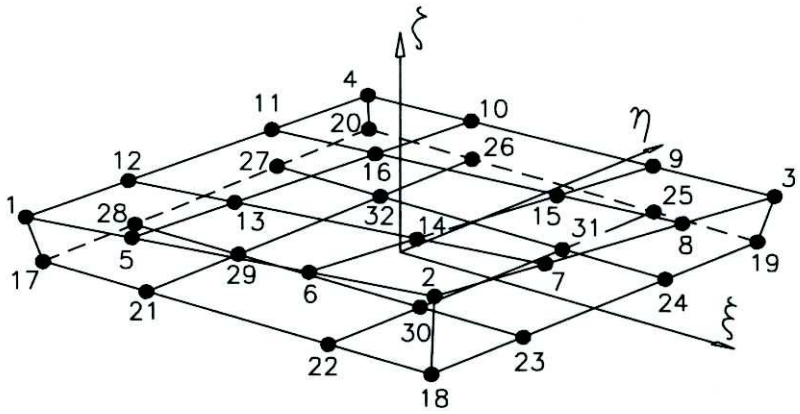

Fig. 1. 32-node finite non zero-thickness foundation element.

According to the last part of Eq. (2), the stiffness matrix of the foundation is given by

$$K_{ij} = k_0 \iint_A N_j N_i \mathrm{d}x\mathrm{d}y + k_1 \iint_A \left(\frac{\partial N_j}{\partial x}\frac{\partial N_i}{\partial x} + \frac{\partial N_j}{\partial y}\frac{\partial N_i}{\partial y} \right) \mathrm{d}x\mathrm{d}y. \tag{17}$$

Following the isoparametric concept, the stiffness submatrices linking nodes i and j of the interface element related to the first k_0 and the second foundation parameter k_1, $(K_0)_{ij}$ and $(K_1)_{ij}$ have the form:

$$(K_0)_{ij} = k_0 \int_{-1}^{+1}\int_{-1}^{+1} N_j N_i \det \mathbf{J}\, d\xi d\eta \tag{18}$$

and

$$(K_1)_{ij} = \int_{-1}^{+1}\int_{-1}^{+1} \frac{k_1}{\det \mathbf{J}} \left(\frac{\partial N_j}{\partial \xi}\frac{\partial y}{\partial \eta} - \frac{\partial N_j}{\partial \eta}\frac{\partial y}{\partial \xi} \right)\left(\frac{\partial N_i}{\partial \xi}\frac{\partial y}{\partial \eta} - \frac{\partial N_i}{\partial \eta}\frac{\partial y}{\partial \xi} \right) d\xi d\eta$$

$$+ \int_{-1}^{+1}\int_{-1}^{+1} \frac{k_1}{\det \mathbf{J}} \left(-\frac{\partial N_j}{\partial \xi}\frac{\partial x}{\partial \eta} + \frac{\partial N_j}{\partial \eta}\frac{\partial x}{\partial \xi} \right)\left(-\frac{\partial N_i}{\partial \xi}\frac{\partial x}{\partial \eta} + \frac{\partial N_i}{\partial \eta}\frac{\partial x}{\partial \xi} \right) d\xi d\eta. \tag{19}$$

It can be readily shown that the components of the Jacobian matrix $\mathbf{J}$ for the finite rectangular elements are constants equal to

$$\mathbf{J} = \begin{bmatrix} \frac{a}{2} & 0 \\ 0 & \frac{b}{2} \end{bmatrix}, \tag{20}$$

where a and b are the lengths of the interface foundation element along the x-axis and y-axis, respectively.

The numerical integration of Eqs. (18) and (19) for the quadrilateral element of rectangular shape with (4×4) sampling points leads to

$$(K_0)_{ij} = \sum_{p=1}^{4}\sum_{q=1}^{4} N_i^T(\xi_p,\eta_q)\, k_0\, N_j(\xi_p,\eta_q) \det \mathbf{J}(\xi_p,\eta_q) W_p W_q \tag{21}$$

and

$$(K_1)_{ij} = \frac{b^2}{4}\sum_{p=1}^{4}\sum_{q=1}^{4} \frac{k_1}{\det \mathbf{J}(\xi_p,\eta_q)} (N_{i,\xi})^2(\xi_p,\eta_q) W_p W_q + \frac{a^2}{4}\sum_{p=1}^{4}\sum_{q=1}^{4} \frac{k_1}{\det \mathbf{J}(\xi_p,\eta_q)} (N_{i,\eta})^2(\xi_p,\eta_q) W_p W_q \tag{22}$$

with W_p and W_q being the integration weights.

Considering the first parameter only and assuming that the finite element nodes overlap the positions of integrating points (this particular process leads to the well-known Lobatto quadrature formulae) we arrive at diagonal (or lumped) stiffness matrices

$$\mathbf{K}_0 = \frac{k_0 ab}{144}\mathrm{diag}[1\ 1\ 1\ 1\ 5\ 5\ 5\ 5\ 5\ 5\ 5\ 5\ 25\ 25\ 25\ 25]. \tag{23}$$

In a similar way we can construct the mass matrix of the plate. From the last integral of the kinetic energy (Eq. (8)) with the help of Eq. (11) (neglecting rotational internal effects), the mass matrix is given by

$$M_{ij} = \rho t \int_{-1}^{+1}\int_{-1}^{+1} N_j N_i \det \mathbf{J} d\xi\, d\eta, \tag{24}$$

which, using the Lobatto 4×4 integration scheme, converts into the non-consistent form

$$\mathbf{M} = \frac{\rho tab}{144}\mathrm{diag}[1\ 1\ 1\ 1\ 5\ 5\ 5\ 5\ 5\ 5\ 5\ 5\ 25\ 25\ 25\ 25], \tag{25}$$

where t is the thickness of the plate.

In practice, diagonal mass matrices are often employed due to their very attractive time-integration schemes in the explicit dynamic methods in which the inversion of the effective stiffness matrix as a linear combination of the damping and mass matrices is required.

3. Foundation parameters

The two parameters k_0 and k_1, in terms of the elastic constants and the dimensions of the plate and the soil foundation, were evaluated by Vallabhan, Straughan and Das in [24]. These parameters applied to a foundation with a finite depth of soil h can be defined by

$$k_0 = \frac{E_0}{(1-\nu_0^2)} \int_0^h \left(\frac{\mathrm{d}\psi(z)}{\mathrm{d}z}\right)^2 \mathrm{d}z \tag{26}$$

and

$$k_1 = \frac{E_0}{2(1+\nu_0)} \int_0^h \psi^2(z)\mathrm{d}z \tag{27}$$

with the mode function $\psi(z)$ which can be described in the following way [24]:

$$\psi(z) = \frac{\sinh\gamma\dfrac{h-z}{h}}{\sinh\gamma}. \tag{28}$$

The generalized modulus of elasticity E_0 and and the Poisson ratio ν_0 are defined by

$$E_0 = \frac{E_f}{1-\nu_f^2}, \qquad \nu_0 = \frac{\nu_f}{1-\nu_f}, \tag{29}$$

where E_f and ν_f are the modulus of elasticity and Poisson's ratio of the foundation, respectively. Using the mode function $\psi(z)$ as given in Eq. (28), the foundation parameters k_0 (Eq. (26)) and k_1 (Eq. (27)) become

$$k_0 = \frac{E_f(1-\nu_f)}{8h(1+\nu_f)(1-2\nu_f)}\frac{2\gamma\sinh 2\gamma + 4\gamma^2}{\sinh^2\gamma} \tag{30}$$

and

$$k_1 = \frac{E_f h}{16\gamma^2(1+\nu_f)}\frac{2\gamma\sinh 2\gamma - 4\gamma^2}{\sinh^2\gamma}. \tag{31}$$

4. Numerical examples

4.1. Free rectangular plate on an elastic Pasternak foundation

A plate of size 9.144×12.192 m and thickness of $t = 0.1524$ m resting on a nonhomogeneous non-layered soil medium, the properties of which can vary linearly in the vertical direction, is investigated first (see Fig. 2). A particular case of this problem in which E_1 is equal to E_2 was considered by Çelik and Saygun [3] and Buczkowski and Torbacki [7]. For comparison with other results, the value of $E_f = E_1 = E_2 = 68950$ kN/m^2 (a sand dense soil) are assumed as those in their works. Here, the

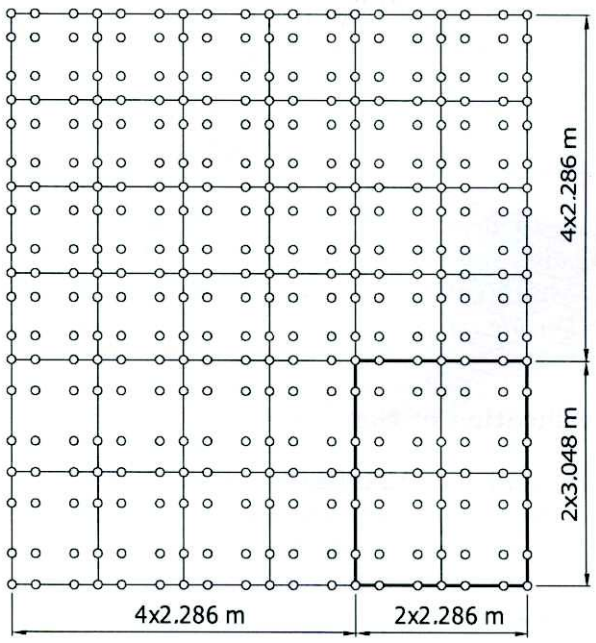

Fig. 2. Free rectangular plate on an elastic foundation (only one quadrant is discretized using 16-node elements). The plate is of size 9.144×12.192 m (the rest is the foundation outside the plate).

depth of the foundation h is equal to 15.240 m with the same values of elastic moduli of the soil E_1 at the top and E_2 at the bottom and a Poisson's ratio equal to $\nu_f = 0.25$ and $\nu_p = 0.20$, respectively, for the soil and plate is used. The elastic modulus of the plate is assumed to be $E_p = 20685$ MPa. The results indicate that for the case of uniformly distributed loads, the plate deflections increase with the depth of the soil. There is an interesting fact to emphasize that the plate deflections for a concentrated load are not significantly different for various depths of soil. The second parameter is responsible for the effect of a membrane underneath the plate which explains why the plate deformations for various depths of soil are just slightly different for this form of loading. From the other side, however, in the case of the concentrated load the values of the foundation parameters k_0 and, in particular, k_1 change (with the depths of soil) to a lesser degree than in the case of uniformly distributed load.

The results lead to the conclusion that the interaction between the plate and the soil depends not only on the values of both the foundation parameters varying with the depth of soil, but also on the distribution of the applied load.

Another way to show the benefits of the proposed method is to use a uniformly loaded plate that has a different thickness t but the same value of the soil depth $h = 15.24$ m.

The ability to handle thin plates on elastic foundation by the 16-node Lagrange Mindlin plate element is illustrated in Table 1. The stable convergence of results for very thin plates up to $b/t = 10^6$ is worth noticing. It is clear that for relatively small values of the plate's thickness and its length, the overall deflection of the plate should be different. However, for larger ratios t the deflection of the plate does not alter.

Table 1. The vertical displacement at the centre of the plate in [mm] for a uniformly distributed load $q = 0.02394$ N/mm^2, $k_0 = 5964$ kN/m^3 (Eq. (30)), $k_1 = 104664$ kN/m (Eq. (31)), $h = 15.240$ m, $b = 12.192$ m (the values of the parameter γ are given in [7]).

b/t	t [mm]	KQ4	MQ16(G)	MQ16(L)	[7]
2	6096	180.49	194.73	194.73	135.84
4	3048	214.44	214.23	214.23	137.37
10	1219.2	220.77	220.64	220.64	153.42
20	609.6	220.96	220.97	220.97	193.50
80	152.4	220.98	221.01	221.00	220.55
100	60.96	220.98	221.01	221.01	220.90
500	24.384	220.98	221.01	221.01	221.04
10^3	12.192	220.98	221.01	221.01	221.04
10^6	0.012192	220.98	221.01	221.01	221.04

KQ4 – 4-node thin plate element based on the Kirchhoff theory, MQ16(G) – 16-node thick Mindlin element with a Gauss integration scheme (the nodes of the element coincide with the Gauss integration points), MQ16(L) – 16-node thick Mindlin element with a Lobatto integration scheme (see Appendix A). For $b/t = 100$, the authors in [3] give the value of 221.2 mm.

4.2. Free vibration – verification of the theory

The presented approach using a 16-node Mindlin element (MQ16(L)) was verified against the results produced by Akhavan et al. [20]. In the study, the authors presented a closed-form analytical solution for free vibration analysis of moderately thick rectangular plates resting on a Pasternak elastic foundation for various combinations of boundary conditions. In the paper, the non-dimensional Winkler foundation coefficient $\overline{k}_0$ is

$$\overline{k}_0 = k_0 \frac{a^4}{D}, \tag{32}$$

where a is the length of plate, D denotes the plate flexural rigidity

$$D = \frac{Et^3}{12(1-\nu^2)} \tag{33}$$

and k_1 is the Winkler foundation coefficient, which was taken as 0 and 1000, while the non-dimensional shear foundation coefficient $\overline{k}_1$

$$\overline{k}_1 = k_1 \frac{a^2}{D} \tag{34}$$

was also taken as 0 and 1000, thus yielding four cases: a plate without an elastic foundation ($\overline{k}_0 = 0$, $\overline{k}_1 = 0$), a plate resting on a Winkler foundation ($\overline{k}_0 = 1000$, $\overline{k}_1 = 0$) and a plate resting on a Pasternak foundation ($\overline{k}_0 = 1000$, $\overline{k}_1 = 1000$).

Regarding the plate, the first-order shear deformation theory was employed to extract an eigenvalue equation yielding the natural frequencies for the moderately thick rectangular plates. The dimensions of the square plate for verification were taken as follows: $a = 1$ m, plate thickness $t = 1$ mm, material properties: Young's modulus $E = 70000$ MPa, Poisson's ratio $\nu = 0.3$ and density $\rho = 2702 \cdot 10^{-9}$ kg/mm^3. The actual values of the Winkler and shear coefficients, corresponding to the non-dimensional value of 1000 for both of them, were $k_0 = 6.41026 \cdot 10^6$ N/mm and $k_1 = 6.410256$ N/mm^3.

The finite element models for various mesh densities are presented in Figs. 3 and 4.

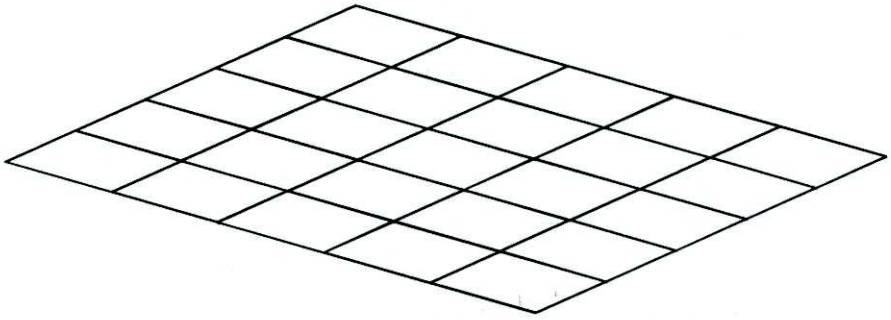

Fig. 3. Model of plate – finite element mesh 5×5.

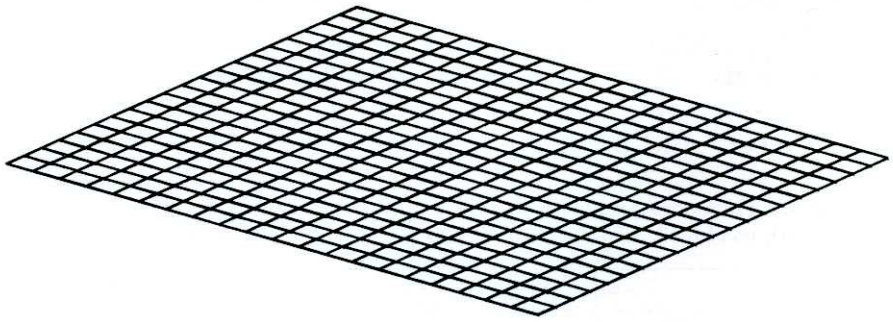

Fig. 4. Model of plate – finite element mesh 20×20.

Results are given in the form of frequency parameters where the actual natural frequency is scaled in the following way:

$$\alpha = \omega a^2 \sqrt{\frac{\rho t}{D}}. \tag{35}$$

The results for simply supported plates (four edges simply supported – SSSS) are shown in Tables 2 and 3.

Table 2. Frequency-scaled parameter α which corresponds to first frequency ω_1 [s^{-1}] for a simply supported plate (SSSS) for various foundation coefficients.

	$\overline{k}_0 = 0,\ \overline{k}_1 = 0$	$\overline{k}_0 = 1000,\ \overline{k}_1 = 0$
Akhavan et al. [20]	19.7391	37.2778
KQ4 5 × 5	19.3471	37.0805
KQ4 20 × 20	19.7129	37.2658
MQ16(G) 5 × 5	19.7401	37.2784
MQ16(G) 20 × 20	19.7384	37.2776
MQ16(L) 5 × 5	19.7402	37.2786
MQ16(L) 20 × 20	19.7386	37.2777

Table 3. Frequency-scaled parameter α which corresponds to first frequency ω_1 [s^{-1}] for a simply supported plate (SSSS) for various foundation coefficients.

	$\overline{k}_0 = 1000,\ \overline{k}_1 = 0$	$\overline{k}_0 = 1000,\ \overline{k}_1 = 1000$
Akhavan et al. [20]	141.876	145.358
KQ4 5 × 5	141.550	145.047
KQ4 20 × 20	141.880	145.363
MQ16(G) 5 × 5	141.879	145.361
MQ16(G) 20 × 20	141.879	145.361
MQ16(L) 5 × 5	141.879	145.362
MQ16(L) 20 × 20	141.879	145.362

The results are also given for a plate with a combination of boundary conditions – SCSF (simple support-clamped-simple support-free). In this case, the results are also given for various foundation coefficients, corresponding to a plate without an elastic foundation and a plate resting on an elastic foundation, of either Winkler or Pasternak type. For the SCSF plates, the results are given for a 20 × 20 mesh in Tables 4 and 5.

Comparisons between the reference and present results prove the high accuracy of the present formulation.

Table 4. Frequency parameter α which corresponds to first frequency ω_1 [s^{-1}] for a plate with combined boundary conditions (SCSF) for various foundation coefficients.

	$\overline{k}_0 = 0,\ \overline{k}_1 = 0$	$\overline{k}_0 = 1000,\ \overline{k}_1 = 0$
Akhavan et al. [20]	12.6862	34.0726
KQ4-node 5 × 5	12.6621	34.1061
KQ4-node 20 × 20	12.6859	34.1065
MQ16(G) 5 × 5	12.6893	34.0970
MQ16(G) 20 × 20	12.6873	34.1009
MQ16(L) 5 × 5	12.6893	34.0977
MQ16(L) 20x20	12.6873	34.1011

Table 5. Frequency parameter α which corresponds to first frequency ω_1 [s^{-1}] for a plate with combined boundary conditions (SCSF) for various foundation coefficients.

	$\bar{k}_0 = 1000, \quad \bar{k}_1 = 0$	$\bar{k}_0 = 1000, \quad \bar{k}_1 = 1000$
Akhavan et al. [20]	113.315	117.645
KQ4-node 5×5	112.596	116.957
KQ4-node 20×20	112.524	116.896
MQ16(G) 5×5	112.665	117.025
MQ16(G) 20×20	112.516	116.885
MQ16(L) 5×5	112.666	117.026
MQ16(L) 20×20	112.517	116.885

5. Concluding remarks

The formulation for bending and natural frequency analysis of plates resting on a two-parameter elastic foundation in the framework of the finite element method was presented in this paper. The problem of the plate resting on an elastic layered foundation was solved using zero-thickness interface elements. The adopted model was employed to analyse thick as well thin plates resting on an inelastic foundation with common boundary conditions and loading combinations. We recommend to use a 16-node Mindlin plate element of the Lagrange family to handle extremely thin plates with very large length-thickness ratios up to $\frac{b}{t} = 10^6$. By employing the Lobatto numerical integration in which the integration points coincide with the element nodes, we obtained the diagonal form of the mass matrix of the plate. Diagonal mass matrices are very attractive for dynamic explicit analyses. The method was developed to also take into account the surrounding effect outside the plate.

A significant influence of the elastic foundation on the natural frequency was observed and the analysed system exhibited the nonlinear response when considering the variation of eigenfrequency for the smaller values of the Winkler coefficient, while the eigenfrequency increased almost linearly for the greater values. The influence of the second coefficient for the investigated range of coefficients was linear. The present results agree quite well with the theoretical and numerical results given by other authors.

Appendix A: The shape functions for the cubic 16-node Mindlin plate element with a Lobatto integration scheme

Derivation of higher-order isoparametric elements is performed with the help of one-dimensional Lagrange polynomials defined by

$$l_a^{n_{en}-1}(\xi) = \frac{(\xi - \xi_1)(\xi - \xi_2)\cdots(\xi - \xi_{a-1})(\xi - \xi_{a+1})\cdots(\xi - \xi_{n_{en}})}{(\xi_a - \xi_1)(\xi_a - \xi_2)\cdots(\xi_a - \xi_{a-1})(\xi_a - \xi_{a+1})\cdots(\xi_a - \xi_{n_{en}})},$$

where a is the node, $n_{en} - 1$ defines the order of the polynomial (n_{en} is the number of nodes in the element) and ξ_a denotes the location of the nodes in ξ – space. In the equation above, the a – term is omitted.

The shape functions for the cubic 16-node element ($n_{en} = 4$) are set up by taking products of the cubic Lagrange polynomials (this procedure is schematically illustrated in Fig. A1). We have, for example, that for node 16 ($\xi_2 = -1/\sqrt{5}$, $\eta_3 = +1/\sqrt{5}$)

$$N_{16} = l_2^3(\xi) l_3^3(\eta),$$

where

$$l_2^3(\xi) = \frac{(\xi-\xi_1)(\xi-\xi_3)(\xi-\xi_4)}{(\xi_2-\xi_1)(\xi_2-\xi_3)(\xi_2-\xi_4)} = \frac{(\xi+1)\left(\xi-\frac{1}{\sqrt{5}}\right)(\xi-1)}{\left(-\frac{1}{\sqrt{5}}+1\right)\left(-\frac{1}{\sqrt{5}}-\frac{1}{\sqrt{5}}\right)\left(-\frac{1}{\sqrt{5}}-1\right)}$$

$$= \frac{5}{8}\left(\sqrt{5}\xi^3-\xi^2-\sqrt{5}\xi+1\right)$$

and

$$l_3^3(\eta) = -\frac{5}{8}\left(\sqrt{5}\eta^3+\eta^2-\sqrt{5}\eta-1\right).$$

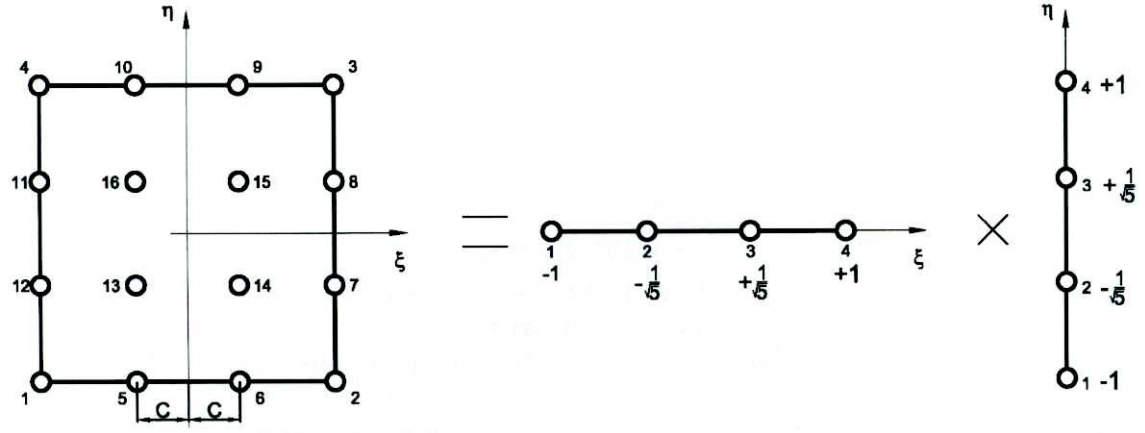

Fig. A1. Node location in ξ–η space for the cubic 16-node element.

In an analogous way, we can obtain all shape functions, which are given by

$$N_1 = \frac{1}{64}\left(5\xi^3-5\xi^2-\xi+1\right)\cdot\left(5\eta^3-5\eta^2-\eta+1\right),$$

$$N_2 = -\frac{1}{64}\left(5\xi^3+5\xi^2-\xi-1\right)\cdot\left(5\eta^3-5\eta^2-\eta+1\right),$$

$$N_3 = \frac{1}{64}\left(5\xi^3+5\xi^2-\xi-1\right)\cdot\left(5\eta^3+5\eta^2-\eta-1\right),$$

$$N_4 = -\frac{1}{64}\left(5\xi^3-5\xi^2-\xi+1\right)\cdot\left(5\eta^3+5\eta^2-\eta-1\right),$$

$$N_5 = -\frac{5}{64}\left(\sqrt{5}\xi^3-\xi^2-\sqrt{5}\xi+1\right)\cdot\left(5\eta^3-5\eta^2-\eta+1\right),$$

$$N_6 = \frac{5}{64}\left(\sqrt{5}\xi^3+\xi^2-\sqrt{5}\xi-1\right)\cdot\left(5\eta^3-5\eta^2-\eta+1\right),$$

$$N_7 = \frac{5}{64}\left(5\xi^3+5\xi^2-\xi-1\right)\cdot\left(\sqrt{5}\eta^3-\eta^2-\sqrt{5}\eta+1\right),$$

$$N_8 = -\frac{5}{64}\left(5\xi^3+5\xi^2-\xi-1\right)\cdot\left(\sqrt{5}\eta^3+\eta^2-\sqrt{5}\eta-1\right),$$

$$N_9 = -\frac{5}{64}\left(\sqrt{5}\xi^3+\xi^2-\sqrt{5}\xi-1\right)\cdot\left(5\eta^3+5\eta^2-\eta-1\right),$$

$$N_{10} = \frac{5}{64}\left(\sqrt{5}\xi^3 - \xi^2 - \sqrt{5}\xi + 1\right)\cdot\left(5\eta^3 + 5\eta^2 - \eta - 1\right),$$

$$N_{11} = \frac{5}{64}\left(5\xi^3 - 5\xi^2 - \xi + 1\right)\cdot\left(\sqrt{5}\eta^3 + \eta^2 - \sqrt{5}\eta - 1\right),$$

$$N_{12} = -\frac{5}{64}\left(5\xi^3 - 5\xi^2 - \xi + 1\right)\cdot\left(\sqrt{5}\eta^3 - \eta^2 - \sqrt{5}\eta + 1\right),$$

$$N_{13} = \frac{25}{64}\left(\sqrt{5}\xi^3 - \xi^2 - \sqrt{5}\xi + 1\right)\cdot\left(\sqrt{5}\eta^3 - \eta^2 - \sqrt{5}\eta + 1\right),$$

$$N_{14} = -\frac{25}{64}\left(\sqrt{5}\xi^3 + \xi^2 - \sqrt{5}\xi - 1\right)\cdot\left(\sqrt{5}\eta^3 - \eta^2 - \sqrt{5}\eta + 1\right),$$

$$N_{15} = \frac{25}{64}\left(\sqrt{5}\xi^3 + \xi^2 - \sqrt{5}\xi - 1\right)\cdot\left(\sqrt{5}\eta^3 + \eta^2 - \sqrt{5}\eta - 1\right),$$

$$N_{16} = -\frac{25}{64}\left(\sqrt{5}\xi^3 - \xi^2 - \sqrt{5}\xi + 1\right)\cdot\left(\sqrt{5}\eta^3 + \eta^2 - \sqrt{5}\eta - 1\right).$$

The shape function matrix $\mathbf{N}^{(2)}$ is expressed as

$$\mathbf{N}^{(2)} = \begin{bmatrix} N_1 & 0 & 0 & N_2 & 0 & \ldots & 0 \\ 0 & N_1 & 0 & 0 & N_2 & \ldots & 0 \\ 0 & 0 & N_1 & 0 & 0 & \ldots & N_{16} \end{bmatrix}.$$

APPENDIX B: PATCH TEST FOR THE 16-NODE MINDLIN PLATE ELEMENT

The ideal Mindlin-type element should [26]: (1) converge, (2) not lock, (3) contain no mechanisms, (4) be capable of providing accurate displacements and stresses, (5) be insensitive to element distortions and (6) be invariant to the direction of the coordinate system.

The benchmark tests may be used to check that the new element satisfies some of the above criteria. However, it is known that correct patch test results are neither sufficient nor necessary conditions for convergence.

Patch tests performed on a plate element with mesh shown in Fig. B1 indicate that the plate element can represent fields of constant moment, twist or shear.

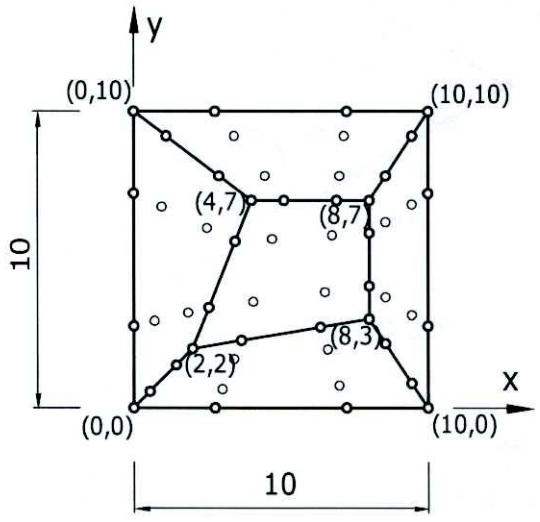

Fig. B1. Patch test mesh formed by a square of 10 × 10 mm, E = 210000 MPa, ν = 0.3, t = 1 mm.

B.1. Patch test for membrane tension

In the membrane patch test shown in Fig. B2 a distributed force of constant intensity equal to $q = 1$ N/mm was applied at the right edge of the plate element. The plate element was clamped at the left edge and boundary conditions were applied to restrain the longitudinal edges in the transverse direction. The result was a uniform stress field in the longitudinal direction as well as a uniform stress field in the transverse direction $\sigma_x = 1$ MPa, with the correct ratio between the stresses corresponding to the Poisson ratio, $\sigma_y = 0.3$ MPa. Therefore, it can be concluded that the results show that the present element passed the test.

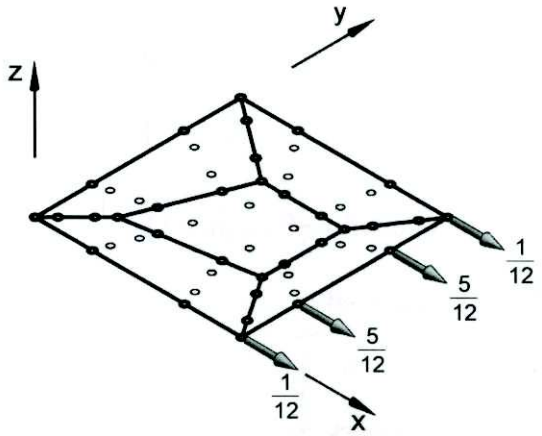

Fig. B2. Patch test for in-plane tension.

B.2. Patch test for bending

In the bending patch test shown in Fig. B3, a distributed edge moment of constant intensity equal to $m = 1$ N·mm/mm was applied at the right edge of the plate element. The left edge was clamped. The result was a uniform stress field $\sigma_x = 6$ MPa, which was corresponding to the analytical solution what confirms that the element passed the test.

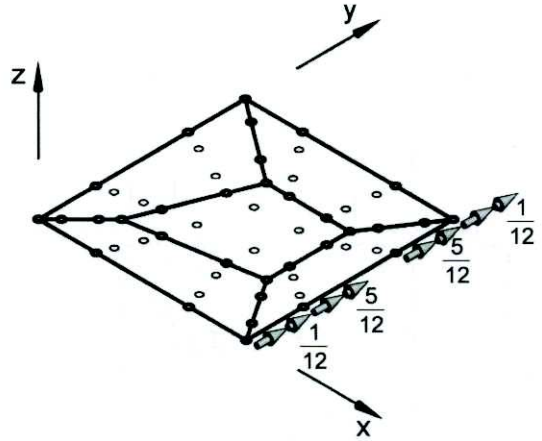

Fig. B3. Patch test for bending.

B.3. Patch test for twisting

The plate element was supported on three corners and loaded with distributed moments of constant intensity equal to $m = 1$ N·mm/mm applied at the edges, meeting at the unsupported point as shown

in Fig. B4. This test was established for Kirchhoff plate elements but is also reasonable for Mindlin plate elements which are very thin. The result was a stress field $\tau_{xy} = 6$ MPa corresponding to the analytical solution. The present element therefore passed the test.

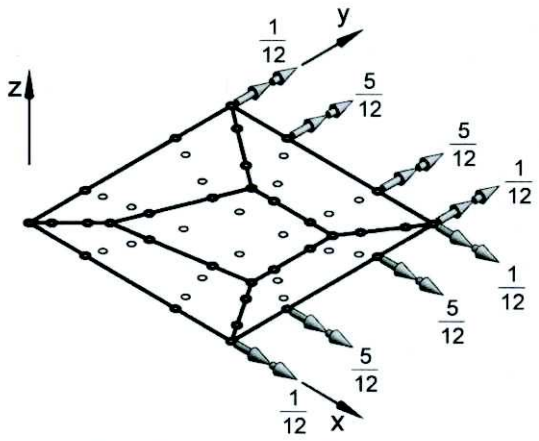

Fig. B4. Patch test for twisting.

B.4. Patch test for shear

In the shear patch test shown in Fig. B5, a lateral distributed edge load of constant intensity equal to $q = 1$ N/mm was applied at the right edge of the element which was fully clamped at the left edge. Additionally, all rotations must be constrained in order to prevent the appearance of a bending moment. The element also passed this test as the uniform shear stress equal to $\tau_{xz} = 1$ MPa was a response to the applied loading.

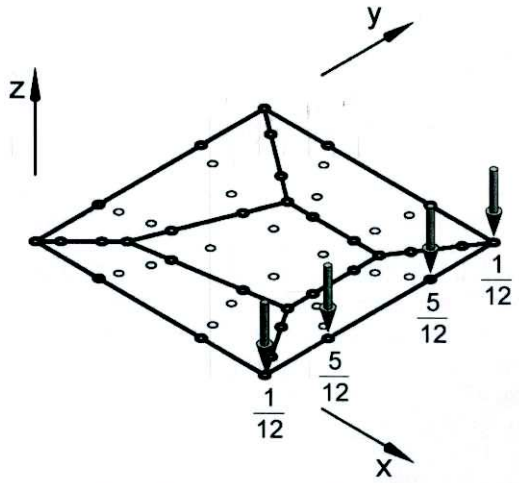

Fig. B5. Patch test for shear.

ACKNOWLEDGMENTS

This work was performed within the scope of project *Static and dynamic finite element analysis of layered structures on elastic nonhomogeneous foundation* [in Polish: *Statyczna i dynamiczna analiza warstwowych konstrukcji płytowych spoczywających na niejednorodnym podłożu sprężystym*] financed by the National Science Centre (Narodowe Centrum Nauki – NCN) of Poland under contract 2012/05/B/ST6/03086. The support is gratefully acknowledged.

REFERENCES

[1] M.H. Omurtag, A. Özütok, A.Y. Aköz. Free vibration analysis of Kirchhoff plates resting on elastic foundation by mixed finite element fomulation based on Gâteaux differential. *Int. J. for Numer. Methods in Eng.*, **40**: 295–317, 1997.

[2] D. Zhou, Y.K. Cheung, S.H. Lo, F.T.K. Au. Three-dimensional vibration analysis of rectangular thick plates on Pasternak foundation. *Int. J. for Numer. Methods in Eng.*, **59**: 1313–1334, 2004.

[3] M. Çelik, A. Saygun. A method for the analysis of plates on a two-parameter foundation. *Int. J. of Solids and Struct.*, **36**: 2891–2915, 1999.

[4] M. Çelik, M. Omurtag. Determination of the Vlasov foundation parameters – quadratic variation of elasticity modulus – using FE analysis. *Structural Engineering and Mechanics*, **19**(6): 619–637, 2005.

[5] K. Ozgan, A.T. Daloglu. Alternative plate elements for the analysis of thick plates on elastic foundation. *Structural Engineering and Mechanics*, **26**(1): 69–86, 2007.

[6] K. Ozgan, A.T. Daloglu. Effect of transverse shear strains on plates resting on elastic foundation using modified Vlasov model. *Thin-Walled Structures*, **46**: 1236–1250, 2008.

[7] R. Buczkowski, W. Torbacki. Finite element modelling of thick plates on two-parameter elastic foundation. *International Journal for Numerical and Analytical Methods in Geomechanics*, **25**(14): 1409–1427, 2001.

[8] R. Buczkowski, W. Torbacki. Finite element analysis of plates on layered tensionless foundation. *Archives of Civil Engineering*, **56**(3): 255–274, 2010.

[9] Z. Celep. Rectangular plates resting on tensionless elastic foundation. *J. of Eng. Mech. ASCE*, **114**(12): 2083–2092, 1988.

[10] Z. Celep, K. Güler. Axisymmetric forced vibrations of an elastic free circular plate on tensionless two parameter foundation. *Journal of Sound and Vibration*, **301**: 495–509, 2007.

[11] R.C. Mishra, S.K. Chakrabarti. Rectangular plates resting on tensionless elastic foundation: some new results. *Journal of Engineering Mechanics ASCE*, **122**(4): 385–387, 1996.

[12] N. Eratll, A.Y. Aköz. The mixed finite element formulation for the thick plates on elastic foundations. *Comput. and Struct.*, **65**(4): 515–529, 1997.

[13] Y. Özçelikörs, M.H. Omurtag, H. Demir. Analysis of orthotropic plate-foundation interaction by mixed finite element formulation using Gâteaux differential. *Comput. and Struct.*, **62**(1): 93–106, 1997.

[14] H.-S. Shen. Nonlinear bending of Reissner-Mindlin plates with free edges under transverse and in-plane loads and resting on elastic foundations. *Int. J. of Mech. Sci.*, **41**: 845–864, 1999.

[15] Y.T. Feng, D.R.J. Owen. Iterative solution of coupled FE/BE discretizations for plate-foundation interaction problems. *Int. J. for Numer. Methods in Eng.*, **39**: 1889–1901, 1996.

[16] L. Sadecka. A finite/infinite element analysis of thick plate on a layered foundation. *Comput. and Struct.*, **76**: 603–610, 2000.

[17] Ö. Civalek, M.H. Acar. Discrete singular convolution method for the analysis of Mindlin plates on elastic foundations. *International Journal of Pressure Vessels and Piping*, **84**: 527–535, 2007.

[18] Ö. Civalek, H. Ersoy. Free vibration and bending analysis of circular Mindlin plates using singular convolution method. *Commun. Numer. Meth. Engrg.*, **25**: 907–92, 2009.

[19] H. Akhavan, Sh. Hosseini Hashemi, H. Rokni Damavandi Taher, A. Alibeigloo, Sh.Vahabi. Exact solutions for rectangular Mindlin plates under in-plane loads resting on Pasternak elastic foundation. Part I: Buckling analysis. *Computational Materials Science*, **44**: 968–978, 2009.

[20] H. Akhavan, Sh. Hosseini Hashemi, H. Rokni Damavandi Taher, A. Alibeigloo, Sh. Vahabi. Exact solutions for rectangular Mindlin plates under in-plane loads resting on Pasternak elastic foundation. Part II: Frequency analysis. *Computational Materials Science*, **44**: 951–961, 2009.

[21] A.M. Zenkour. Bending of orthotropic plates resting on Pasternak's foundations using mixed shear deformation theory. *Acta Mechanica Sinica*, **27**(6): 956–962, 2011.

[22] A.M. Zenkour, M.N.M. Allam, M.O. Shaker, A.F. Radwan. On simple and mixed first-order theories for plates resting on elastic foundations. *Acta Mech.*, **220**: 33–46, 2011.

[23] A.M. Zenkour, M.N.M. Allam, M. Sobhy. Bending of a fiber-reinforced viscoelastic composite plate resting on elastic foundations. *Arch. Appl. Mech.*, **81**: 77–96, 2011.

[24] V.G. Vallabhan, A.T. Daloglu. Consistent FEM-Vlasov model for plates on layered soil. *Journal of Structural Engineering ASCE*, **125** (1): 108–113, 1999.

[25] Y.I. Özdemir. Development of a higher order finite element on a Winkler foundation. *Finite Elements in Analysis and Design*, **48**: 1400–1408, 2012.

[26] H.-Ch. Huang. *Static and dynamic analyses of plates and shells*, Springer, Berlin, 1989.